

Intraparticle Surface Plasmon Coupling in Quasi-One-Dimensional Nanostructures

Sungwan Kim,[†] Kevin L. Shuford,[‡] Hye-Mi Bok,[†] Seong Kyu Kim,^{*,†} and Sungho Park^{*,†,§}

Department of Chemistry, BK21 School of Chemical Materials Science, and SKKU Advanced Institute of Nanotechnology, Sungkyunkwan University, Suwon 440-746, South Korea, and Chemical Sciences Division, Oak Ridge National Laboratory, P.O. Box 2008 MS6142, Oak Ridge, Tennessee 37831

Received October 12, 2007; Revised Manuscript Received January 17, 2008

ABSTRACT

The optical properties of two-component quasi-one-dimensional nanostructures consisting of Au and Ni blocks have been investigated. The optically inactive component Ni plays a relaying role in the surface plasmon coupling both for the dipole mode and for the higher-order modes of gold blocks. The experimental results exhibit that the free electrons in Ni participate in the optical coupling phenomenon and that plasmon excitations in the Au blocks induce the free electrons in Ni to oscillate.

Surface plasmons (SPs) are collective oscillations of loosely bound electrons on a metal surface resulting from an interaction with light.¹ The resonance condition depends on the size, shape, composition, and dielectric constants of the metal and the surrounding medium.^{1–3} Metal nanoparticles display unique optical properties, and thus have stimulated intensive research in the use of SPs for a plethora of optical and biomedical applications.^{4–9} Among them, quasi-one-dimensional (1D) nanostructures have exhibited exceptional optical properties compared to other shaped nanoparticles in terms of controllability of SPs,^{10,11} multiplex analyte sensing,¹² and unidirectional plasmon propagation.^{13,14} The control of these 1D nanostructures into ordered assemblies and an understanding of the collective optical properties are critical for enhancing their functional applications. Here we report an intraparticle SP coupling in 1D nanostructures consisting of a 1D array of nanofabricated Au–Ni blocks. The optical properties vary as a function of each block length, and the total length of the structure. Significantly, the optically inactive component Ni plays a relaying role in the SP coupling not only for the dipole mode but also for the higher-order modes of Au blocks.

Our strategy for generating multiblock 1D nanostructures employs the electrochemical deposition of two types of

materials into pores of anodized aluminum oxide (AAO) templates, one (Au) that is optically active in visible–near-IR spectral window and one (Ni) that is inactive in that frequency range. Here, “optically active” or “optically inactive” means whether it shows SPs in the given frequency range. When there are noticeable SPs, we define it as “optically active”. The length of each block can be controlled down to 5 nm by monitoring the charge passed during the electrochemical deposition step.¹⁵ The diameter of a 1D nanostructure depends on the pore diameter of the AAO template utilized, and here templates with a pore diameter of 83 ± 5 nm have been used. In this size regime, the 1D nanostructures exhibit higher-order, longitudinal SP (LSP) resonances that oscillate parallel to the long axis of the rod, as well as a dipolar transverse SP (TSP) mode that oscillates parallel to the short axis.

We synthesized single-component 1D Au nanostructures with different lengths ranging from 120 to 800 nm, and measured their corresponding visible–near-IR extinction spectra (Figure 1). Field emission scanning electron microscopy (FESEM) images reveal their narrow size distribution and homogeneous morphology. As expected, the TSP mode around 550–600 nm is largely insensitive to the increasing aspect ratio showing only a slight blue shift; however, the LSP modes red shift considerably. One noticeable feature is the appearance of multiple peaks beyond 600 nm when the length exceeds $L \sim 250$ nm, which correspond to higher-order LSP modes. The shoulder at 625 nm (Figure 1, spectrum d) moves toward longer wavelengths and develops into the discernible peak at 1060 nm (Figure 1, spectrum g)

* Corresponding authors. E-mail: Seong Kyu Kim (skkim@skku.edu), Sungho Park (spark72@skku.edu).

[†] Department of Chemistry, BK21 School of Chemical Materials Science, Sungkyunkwan University.

[‡] Chemical Sciences Division, Oak Ridge National Laboratory.

[§] SKKU Advanced Institute of Nanotechnology, Sungkyunkwan University.

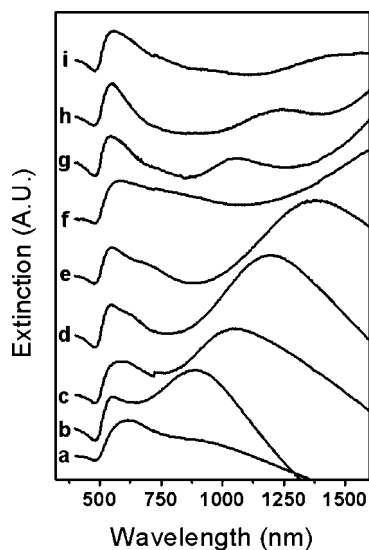


Figure 1. Visible-near-IR extinction spectra of (a) 120, (b) 180, (c) 210, (d) 250, (e) 330, (f) 400, (g) 550, (h) 700, (i) 800 nm long Au 1D nanostructures in D₂O. All the spectra are normalized to have the same extinction for the TSP modes.

as the aspect ratio increases. The red shifts have been observed previously in lithographically generated patterns¹⁶ and the colloidal suspension of Au nanorods.¹⁷ As noted previously, the observation of multiple resonances indicates the high quality of the synthesized 1D nanostructures.¹⁷

A thin layer (ca. 20 nm) of Ni was incorporated into Au blocks to investigate the SP coupling (Figure 2). FESEM images show the Ni block with a dark stripe. When the Ni block is either in the center or at one side of the Au nanorods (the total length ~ 260 nm, Figure 2, panels A and B, respectively), their corresponding spectra (Figure 2, panel E, spectra a and b, respectively) are very similar to single-component Au nanorods ($L \sim 260$ nm). We have calculated

the spectrum (dashed trace, Figure 2E) for the nanostructures in Figure 2A using the discrete dipole approximation (DDA) and obtain good agreement with the experiment. Obviously, the spectrum exhibits characteristics strikingly similar to the single-component Au nanorod spectrum (Figure 1, spectrum d) rather than the linear combination of optical spectra from two Au blocks. The dipole LSP mode at 1210 nm and the higher-order LSP mode at 630 nm are the characteristic features of $L \sim 260$ nm Au nanorods. A single-component $L \sim 120$ nm Au rod shows only a weak dipole LSP mode at ca. 860 nm (Figure 1, spectrum a). An additional feature is the appearance of a higher-order LSP resonance when two short Au blocks are connected by a thin layer of Ni. As shown in Figure 1, the minimum length of solid Au rods that generate these features is ca. 250 nm. Significantly, the presence of a thin Ni block does not perturb the optical coupling of the two Au blocks, and leads to a red shift of the dipole LSP mode as well as the appearance of higher-order LSP modes. Also, the placement of the thin Ni block (center or off center) does not significantly affect the resonance structure. To our knowledge, this is the first observation of two spatially separated units contained within a single nanoparticle that optically couple in a cooperative fashion consistent with the response of a single-component entity. This effect is also observed in longer 1D multiblock Au-Ni-Au nanostructures. The Au-Ni (20 nm)-Au multiblock nanorods with total average lengths, $L \sim 360$ and $L \sim 510$ nm, show an optical spectrum similar to their corresponding single-component Au nanostructures, as is evident by the similarities of Figures 1 and 2. A higher-order LSP mode in Au-Ni-Au nanorods with $L \sim 510$ nm (Figure 2, panel E, spectrum d) appears at 950 nm. Its presence at this wavelength demonstrates that LSPs that mimic the response of a solid Au rod of the summed length can be generated from two shorter Au blocks connected by

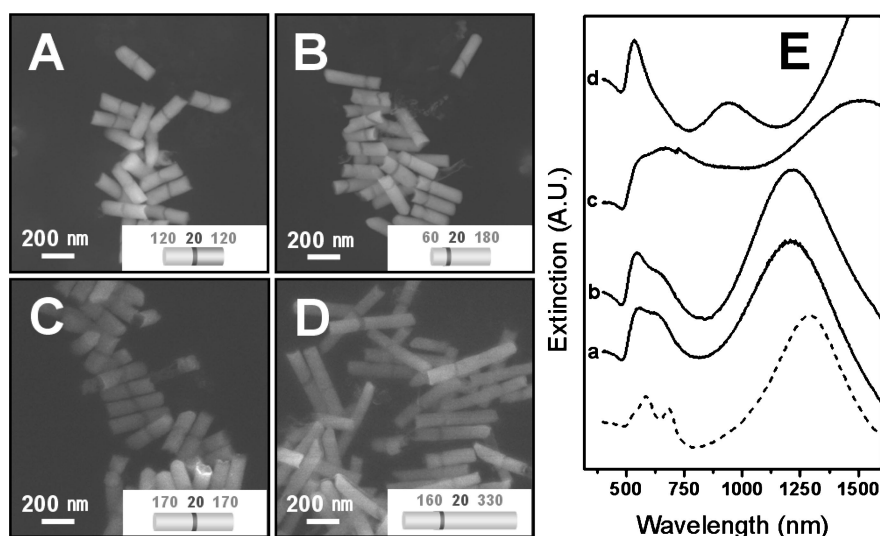


Figure 2. FESEM images of multiblock Au/Ni 1D nanostructures. Total average lengths are (A) 260, (B) 260, (C) 360, and (D) 510 nm. The insets show the dimensions of each block, bright block for Au and dark block for Ni, where the numbers represent the length in nanometer. (E) Visible-near-IR extinction spectra corresponding to the FESEM images. Spectrum a was obtained from the sample shown in image (A), (b) to (B), (c) to (C), and (d) to (D), respectively. The dashed trace is the calculated spectrum for the nanostructures in panel A.

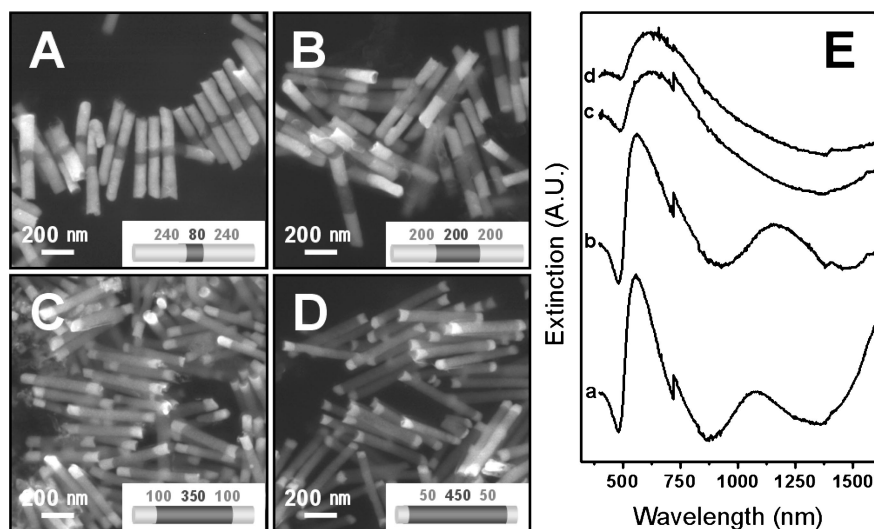


Figure 3. Similar to Figure 2, but for the different lengths for Au and Ni blocks. The average total lengths are (A) 560, (B) 600, (C) 550, and (D) 550 nm. The abrupt features around 700 nm are from lamp and detector changes in the instrument and may obscure weak resonances in this region.

a thin layer of Ni block. There is no intermixing between Au and Ni blocks. When the Au–Ni–Au blocks were immersed in acidic solution (pH ~ 2.5), the Ni blocks were selectively etched out. Their visible–near-IR spectrum reflected that of shorter single-component Au nanorods.

The roles of Ni blocks and the Au block SP coupling were further evaluated by systematically varying the Ni block length within a fixed total 1D nanostructure dimension. In a typical experiment, the 1D nanostructure total length was fixed to be ca. 550–600 nm and the Ni block length was altered to be 80, 200, 350, and 450 nm. Their corresponding FESEM images are represented in Figure 3, panels A–D, respectively. The dark regions illustrate Ni domains and the two bright domains indicate Au blocks. The size distributions of total length and each block length are within 10% of each average length. The spectrum of Au–Ni (80 nm)–Au 1D nanostructures (corresponding to the Figure 3A) is represented in Figure 3, panel E, spectrum a. The two Au end blocks are $L \sim 240$ nm. Surprisingly, there is the distinctive appearance of the higher-order LSP mode centered at 1080 nm. The dipole LSP mode is beyond the observable wavelength limit (1600 nm), but the tail of the dipole band is clearly evident around 1600 nm. The profile of the spectrum is again quite similar to single-component Au 1D nanostructures as shown in Figure 1. If the two Au nanorods (each block length is ~ 240 nm) interact to the maximum extent and the Ni plays no role, one might expect the visible–near-IR spectrum will be the same as one of Au nanorods with a total length ~ 480 nm. In this case, there should be a higher-order LSP mode at ~ 900 nm. However, the mode appears at ~ 1080 nm and the profile of the spectrum is similar to that of a solid Au rod with $L \sim 560$ nm. This suggests that the free electrons in Ni actively participate in the optical coupling phenomenon and that plasmon excitations in the Au blocks induce the free electrons in Ni to oscillate. This hypothesis was further supported by the spectrum represented in Figure 3, panel E, spectrum b, which corresponds to the FESEM image, Figure 3B. The

Ni block length is ~ 200 nm and the two Au blocks are ~ 200 nm (the total $L \sim 600$ nm). There is the clear appearance of the higher-order LSP mode at 1150 nm, consistent with a Au rod with $L \sim 600$ nm. Again we observe a similar situation, where the two Au blocks do not act as one 400 nm rod (Figure 1, spectrum f), but instead generates a spectrum similar to that of a 600 nm Au rod. This suggests that rods with Au blocks separated by as much as 200 nm of Ni still respond essentially as if they were solid Au nanorods. We further increased the Ni block length to 350 nm separating two Au blocks ($L \sim 100$ nm) at the ends. The corresponding spectrum is shown in Figure 3, panel E, spectrum c. As is clearly evident, there is no higher-order LSP mode at ~ 1100 nm as in the other cases, and the peak position of the TSP mode is slightly red shifted. In solid metallic rods, such a shift of the TSP mode is consistent with a scatterer whose rod length has been decreased. In addition, it can be seen that the spectrum profile is similar to that of single-component Au nanorods with a total length $L \sim 100$ nm. The similar spectral behavior was observed when the Ni block length was further increased to be 450 nm, as shown in Figure 3, panel E, spectrum d. This experimental observation elucidates that the Au cannot induce the free electrons in long Ni blocks to oscillate in phase and therefore the single optical contribution from isolated Au blocks is the resulting phenomenon.

We have calculated the optical properties of the block nanorods using DDA. Figure 4 shows the calculated extinction spectra of several particles. Panel A displays the spectrum for a $L = 550$ nm block rod with $L = 265$ nm Au ends separated by 20 nm of Ni. It can clearly be seen in the figure that the Ni block has little effect on the optical spectrum. A solid Au rod (red line) generates almost exactly the same spectrum as the block structure (blue line). This indicates that a small Ni block does not significantly disrupt the longitudinal resonances that are associated with a $L = 550$ nm solid Au rod. There is no noticeable feature in the block structure that can be exclusively attributed to the

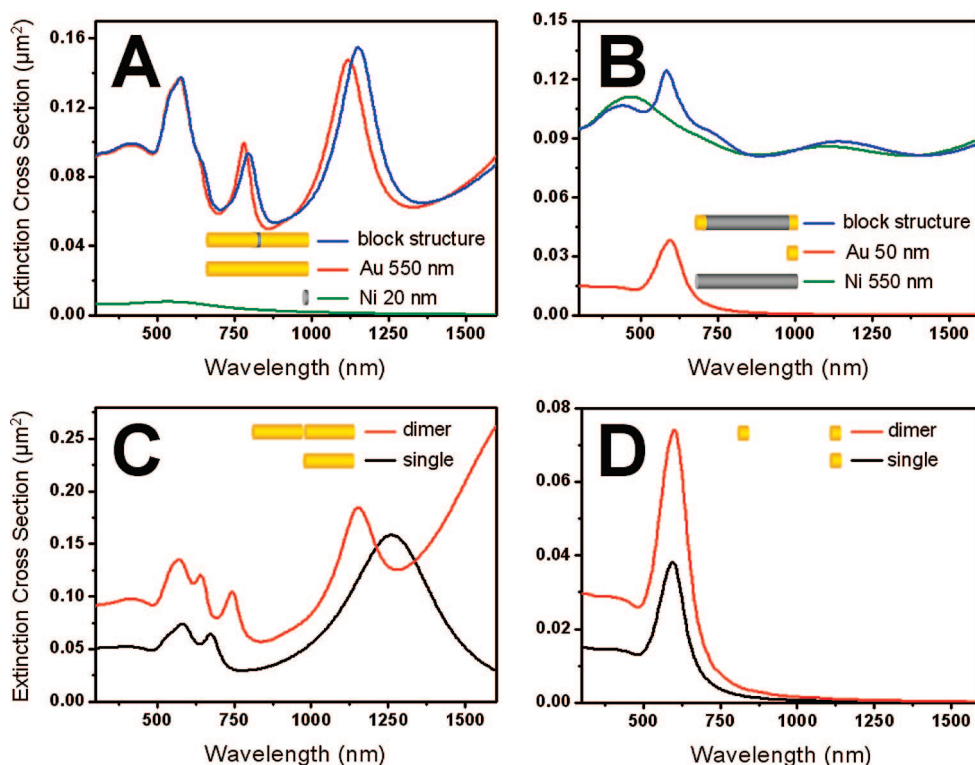


Figure 4. Calculated extinction spectra. (A) and (B) show the extinction spectra of the 1D nanostructures corresponding to the samples described in each panel. (C) and (D) show the extinction spectra equivalent to the nanostructures described in (A) and (B), except the Ni has been removed and replaced by vacuum. (C) Spectra of a single $L = 265$ nm Au rod and a dimer of $L = 265$ nm Au rods separated by 20 nm. (D) Spectra of a single $L = 50$ nm Au rod and a dimer of $L = 50$ nm rods separated by 450 nm.

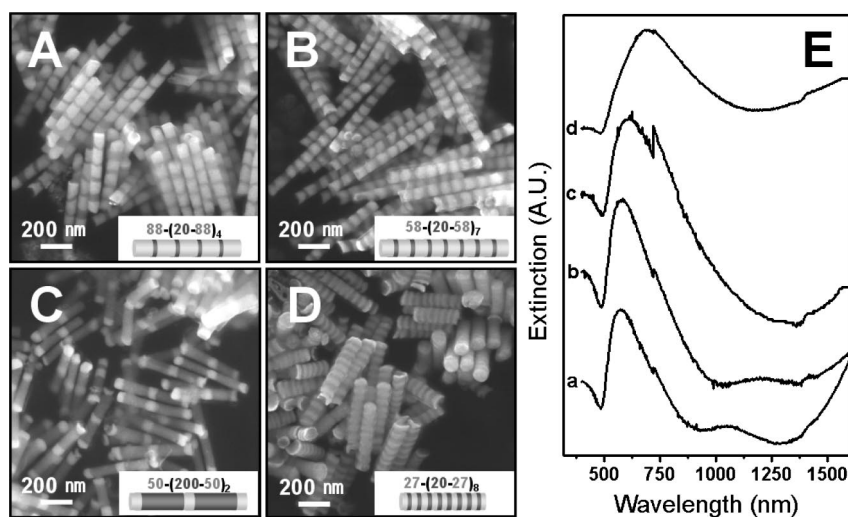


Figure 5. Similar to Figure 2, but for the different lengths and repeating units for Au and Ni blocks. The average total lengths are (A) 520, (B) 600, (C) 550, and (D) 400 nm.

presence of Ni as can be seen by viewing the spectrum for the 20 nm Ni rod. Figure 4B shows the calculated spectrum for a $L = 550$ nm block rod with $L = 50$ nm Au ends separated by $L = 450$ nm of Ni. Also plotted are the spectra for solid rods of Ni and Au with lengths 550 and 50 nm, respectively. The most intense feature for the block structure at ~ 600 nm can be directly attributed to the $L = 50$ nm Au sections on the ends, as is implied by the distinct similarities between the blue and red traces. This also indicates that the Au sections are not coupled to one another and act as single particles. Panels C and D of Figure 4 compare the spectrum

of Au dimers to that of single nanorods. The end-to-end assembly of Au nanorods induces a red shift of the dipole LSP modes.^{18,19} The dimer structures are equivalent to the block nanorods in panels A and B, except the Ni has been removed and replaced by vacuum. Strong coupling is evident in panel C, where the two $L = 265$ nm Au rods are separated by only 20 nm. Several new peaks appear for the dimer structure when compared to the single particle result, the most important of which is the conspicuous feature beyond 1600 nm. Resonances at these wavelengths are associated with much longer nanorods and indicate that the short

nanorods are indeed strongly coupled. Panel D is representative of the opposite extreme. Both the dimer and single particle generate the same spectrum with a single peak at ~ 600 nm. The amplitude of the dimer is twice that of the single particle demonstrating that the individual particles composing the dimer are acting independently. We should note that the calculations presented are for dimers aligned end to end and have been orientationally averaged in the same manner as the single particle results to allow the most direct comparison. In reality this treatment of the dimers represents a somewhat contrived system, as particles in solution do not have a fixed orientation. Regardless, the results do allow us to glean knowledge about the relative distances that are important for Au rods to couple strongly to one another, and hypothesize about the potential role that Ni sections play in block nanorods. The spectral differences between the block nanorods in panels A and B and the dimers in panels C and D indicate that the Ni permits the block rods to function as a single entity and does not merely act as an inert spacer for the two Au blocks. When the Ni block is short, it seamlessly bridges the gap between the Au sections and contributes to the plasmonic behavior without disrupting the original resonance structure. When the Ni block is large, the block rod takes on the characteristics of a solid Ni structure but also does show the contributions from small Au sections. It should be noted that certain metals generate much more intense resonances at these frequencies and that the resonances associated with weakly plasmonic metals such as Ni may be unable to be resolved optically. This is why our experimental results reflect the plasmon resonances associated with Au almost exclusively.

Obviously, the multiblock 1D structures with repeating units of Au–Ni–Au are of great interest to see how the optical coupling characteristics of such structures will vary as a function of each block length and block combination. We synthesized Au–(Ni–Au)₄ with a Au length of $L \sim 88$ nm and a Ni length of ~ 20 nm. The total length is $L \sim 520$ nm. Their FESEM image and the corresponding spectrum are shown in Figure 5, panel A and panel E, spectrum a, respectively. Again, the optical spectrum is quite similar to one from single-component Au 1D nanostructures, showing the higher-order LSP mode at 1050 nm with the dipole LSP mode at a longer wavelength. We decreased Au block length to 58 nm and increased the number of repeating units, that is Au–(Ni–Au)₇, as shown in Figure 5B. Their corresponding spectral features still followed the similar spectral profile of single Au 1D structure (length ~ 600 nm). However, the multiblock 1D nanostructures with shorter Au blocks showed no optical coupling, as evident in Figure 5, panel E, spectra c and d. These results are consistent with the discussion in the preceding paragraph.

This study has introduced the concept of using Ni segments to control the optical coupling of Au blocks in 1D arrays. It has shown that one can systematically make different architectures by controlling the composition of the rod structures and the relative ratio of the blocks of different metals. Insight into such 1D nanostructures not only introduces a new class of materials for optical devices but also is critical to understanding optical coupling in nanostructures. The result of this study should be relevant to the design of plasmon waveguides and highly sensitive chemical and biomedical sensors.

Acknowledgment. This work was supported by the Korea Research Foundation Grant funded by the Korean Government (MOEHRD, KRF-2005-005-J11902, and KRF-C00050) and the Korea Science and Engineering Foundation (R01-2006-000-10426-0-2006). S. K. Kim thanks the KOSEF-SRC program (Center for Nanotubes and Nanostructured Composites). K.L.S. was supported by the Wigner Fellowship Program and the Division of Chemical Sciences, Biosciences, and Geosciences, Office of Basic Energy Sciences, U.S. Department of Energy under Contract DE-AC05-00OR22725 with Oak Ridge National Laboratory, managed and operated by UT-Battelle, LLC.

Supporting Information Available: FESEM images of pure Au 1D nanostructures, EDS analysis of Au–Ni–Au 1D nanostructure and their corresponding visible–near-IR extinction spectra before and after chemical etching of Ni blocks, and details of DDA calculations. This material is available free of charge via the Internet at <http://pubs.acs.org>.

References

- (1) Barnes, W. L.; Dereux, A.; Ebbesen, T. W. *Nature* **2003**, *424*, 824.
- (2) Bohren, C. F.; Huffman, D. R. *Absorption and Scattering of Light by Small Particles*; John Wiley: New York, 1983.
- (3) Henglein, A. *Chem. Rev.* **1989**, *89*, 1861.
- (4) Daniel, M.-C.; Astruc, D. *Chem. Rev.* **2004**, *104*, 293.
- (5) Mirkin, C. A.; Letsinger, R. L.; Mucic, R. C.; Storhoff, J. J. *Nature* **1996**, *382*, 607.
- (6) Elghanian, R.; Storhoff, J. J.; Mucic, R. C.; Letsinger, R. L.; Mirkin, C. A. *Science* **1997**, *277*, 1078.
- (7) Rosi, N. L.; Mirkin, C. A. *Chem. Rev.* **2005**, *105*, 1547.
- (8) Sonnichsen, C.; Reinhard, B. M.; Liphardt, J.; Alivisatos, A. P. *Nat. Biotechnol.* **2005**, *23*, 741.
- (9) Linden, S.; Kuhl, J.; Giessen, H. *Phys. Rev. Lett.* **2001**, *86*, 4688.
- (10) Li, T. J. *J. Phys. Chem. B* **2005**, *109*, 13857.
- (11) Prescott, S. W.; Mulvaney, P. J. *Appl. Phys.* **2006**, *99*, 123504.
- (12) Yu, C.; Irudayaraj, J. *Anal. Chem.* **2007**, *79*, 572.
- (13) Dickson, R. M.; Lyon, L. A. *J. Phys. Chem. B* **2000**, *104*, 6095.
- (14) Ditlbacher, H. *Phys. Rev. Lett.* **2005**, *95*, 257403.
- (15) Qin, L.; Park, S.; Huang, L.; Mirkin, C. A. *Science* **2005**, *309*, 113.
- (16) Krenn, J. R. *Appl. Phys. Lett.* **2000**, *77*, 3379.
- (17) Payne, E. K.; Shuford, K. L.; Park, S.; Schatz, G. C.; Mirkin, C. A. *J. Phys. Chem. B* **2006**, *110*, 2150.
- (18) Aizpurua, J. *Phys. Rev. B* **2005**, *71*, 235420.
- (19) Jain, P. K.; Eustis, S.; El-Sayed, M. A. *J. Phys. Chem. B* **2006**, *110*, 18243.

NL0726353